COMSTAR Experiment:

The Crawford Hill 7-Meter Millimeter Wave Antenna

By T. S. CHU, R. W. WILSON, R. W. ENGLAND, D. A. GRAY,
and W. E. LEGG

(Manuscript received January 27, 1978)

A 7-meter offset Cassegrainian antenna with a precise surface has been built and tested. Measurements using a terrestrial source were made and compared with calculations for 19, 28.5, and 99.5 GHz. Low sidelobe level ($\lesssim -40$ dB) at one degree off the main beam and low cross polarization (≤ -40 dB) throughout the main beam are achieved using a quasi-optical 19/28.5-GHz feed system that also demonstrates very low multiplexing loss (~ 0.1 dB). The prime-focus gain measurement at 99.5 GHz found the difference between the measured and calculated gains to be (0.79 ± 0.45) dB, which is consistent with the expected rms surface error (~ 0.1 mm). Multiple-beam operation accommodates both propagation experiments with the COMSTAR beacons at 19 and 28.5 GHz and millimeter wave radio astronomy observations without physical disturbance of equipment.

I. INTRODUCTION

The Crawford Hill 7-meter antenna (Fig. 1) was built for propagation measurements with the COMSTAR beacons at 19 and 28.5 GHz, and for radio astronomy at frequencies from 70 to 300 GHz. It demonstrates that low sidelobes and high cross-polarization rejection can be obtained in an earth station antenna serving several satellites simultaneously. The antenna will also serve as a test bed for future propagation and antenna measurements.

The main part of this paper is contained in the following three sections. Section II describes the 7-meter antenna starting with the initial requirements. Section III gives a detailed description of the 19/28.5-GHz
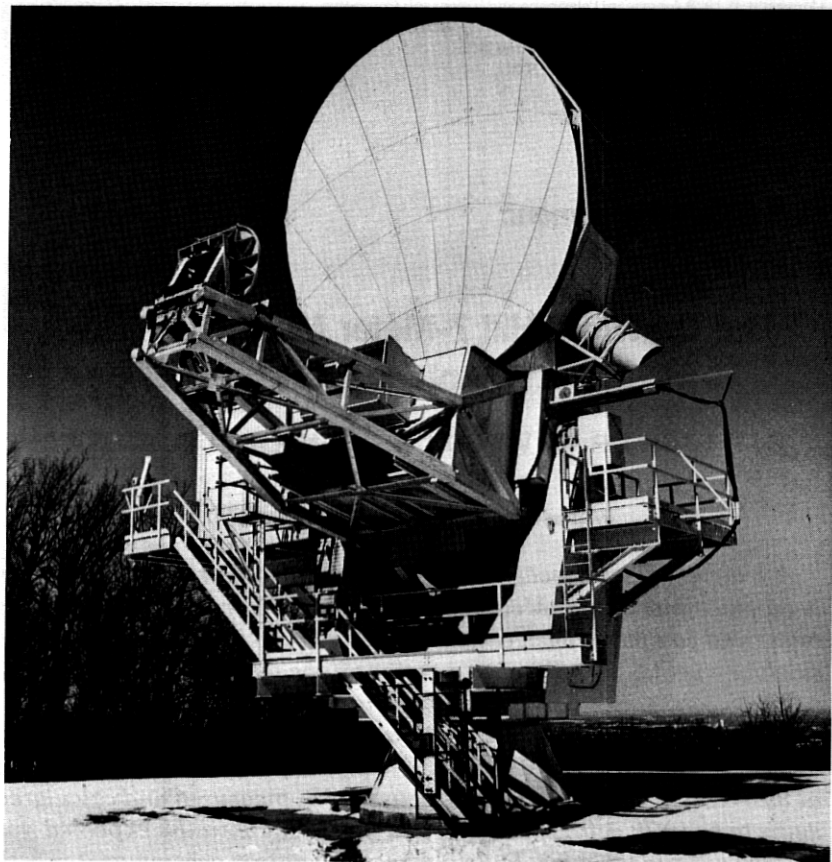
Fig. 1—The 7-meter offset Cassegrainian millimeter wave antenna. The subreflector is mounted below antenna aperture, and key structural parts are covered with insulation.

feed system for the COMSTAR beacon experiment. Section IV describes measurements of the completed antenna at 19, 28.5, and 99.5 GHz using terrestrial sources on a tower at a distance of 11 km.

II. DESCRIPTION

2.1 Requirements

The major requirements imposed by the satellite beacon experiment on the 7-m antenna are for cross polarization to be less than −35 dB within the main beam, sidelobes to be below −40 dB at 1 degree or more from the main beam, multi-beam operation to be possible, and performance in all weather to be good, especially during summer thunder

showers. The attainment of at least minimal performance at the high end of the radio astronomy band further requires a surface accuracy of 0.1-mm rms and a maximum pointing error of 10″ arc. The expectation of performing beam-feed experiments and of possibly accommodating large cryogenically cooled radio astronomy receivers made it desirable to provide for a Nesmyth focus (feed along the elevation axis) in addition to the Cassegrainian focus.

The requirements for low sidelobes imposes severe limitations on the amount of aperture blocking that can be tolerated.[1] Thus, an offset paraboloid was chosen with almost no aperture blockage. This can be made compatible with the cross-polarization and multibeam requirements by choosing a sufficiently large secondary focal ratio.[2,3,4] An additional benefit of the offset design is a large return loss. The low sidelobe requirements also place restrictions on the allowable surface errors. The magnitude of the allowable errors depends on their correlation lengths and the angles at which sidelobes can be tolerated, but a tolerance of about 0.01λ is needed to avoid degradation of the far sidelobes.[5] Thus a surface tolerance of 0.1-mm rms was chosen to simultaneously satisfy the sidelobe requirements at 30 GHz and allow radio astronomical operation in the 200 to 300 GHz band.

The main reflector has a focal length of 6.5659 m. It is offset such that its bottom is 1.2074 m above the reflector axis. The subreflector is a 1.2-m by 1.8-m oval portion of a hyperboloid offset 8.258 cm above its axis (Fig. 2). It has focal lengths of 0.8697 m and 5.2262 m giving a magnification ratio of 6.01. The central ray from the feedhorn to the subreflector makes an angle of 6.828 degrees with the axis and the illumination cone has a half angle of 5.06 degrees. The main reflector is subtended by a circular cone of 26.75-degree half angle, and the axis of the cone makes an offset angle of 37.26 degrees with the axis of the main reflector. The geometry results in a blocking of 4.4 cm of the main reflector by the subreflector and an expected contribution to the cross-polarization level of −56 dB in the main beam region, well below the required level.

The narrow beam pattern required for the feed is the main price which must be paid for the advantages of a large effective F/D ratio. Small-cone-angle corrugated horns have been rejected for both radio astronomy and propagation feeds because of their excessive length. In the radio astronomy feed, cryogenically cooled receivers are in use, and the best performance is obtained by cooling the feedhorn with the receiver and radiationally coupling out of the Dewar. Thus, a small-cone-angle horn would not only be a large mass to cool, but a large low-loss Dewar window would be difficult to make. Instead, a quasi-optical feed system[6] is used for radio astronomy to couple a small corrugated horn in the receiver Dewar to the 7-meter antenna. This feed system incorporates image rejection, local oscillator injection, and calibration.
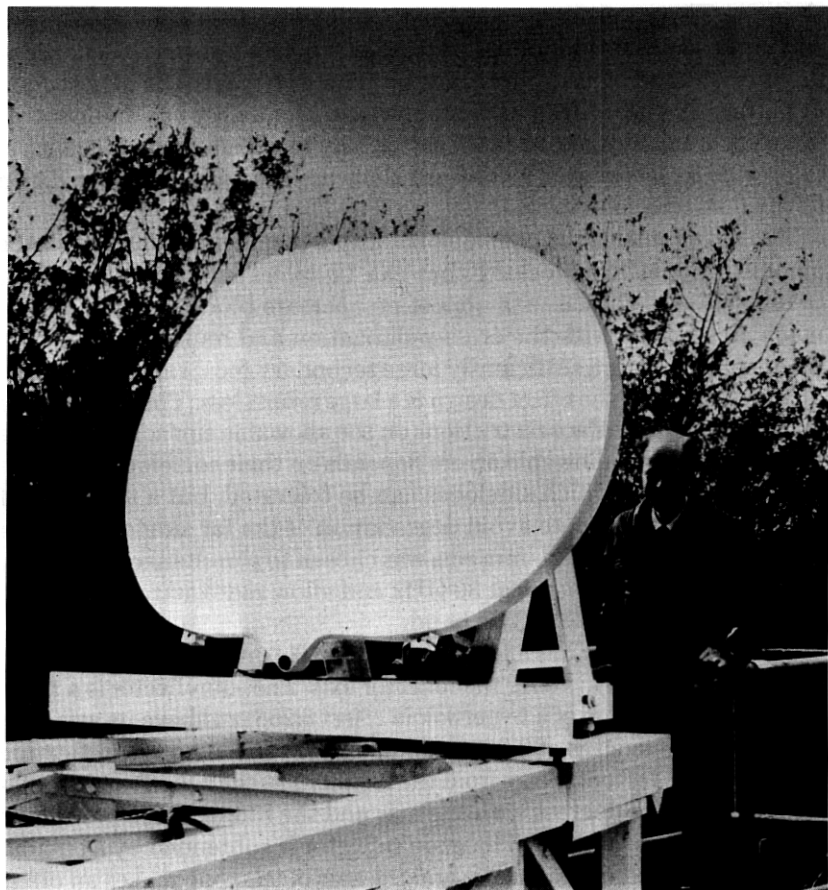
Fig. 2—The subreflector with a machined aluminum surface of 20 μm rms. The oval shape is provided for azimuthal off-axis beams.

In the case of the 19/28.5-GHz propagation feed, the two widely separated frequencies would lead to problems with frequency-dependent phase patterns of a single corrugated feed and with higher order modes generated in a low-loss waveguide polarization diplexer. These problems were circumvented by using quasi-optical methods[7] for both polarization and frequency diplexing as shown in Fig. 3. Four launchers, each consisting of an offset ellipsoid and a corrugated horn, are used, each for a single frequency and polarization. A quasi-optical frequency diplexer[8] first combines two frequencies at each polarization, then a polarization grid[9] combines and simultaneously cleans the two orthogonal polarizations. A 45-degree mirror finally reflects the combined beam to the subreflector, leaving adjacent areas in the focal plane available for other
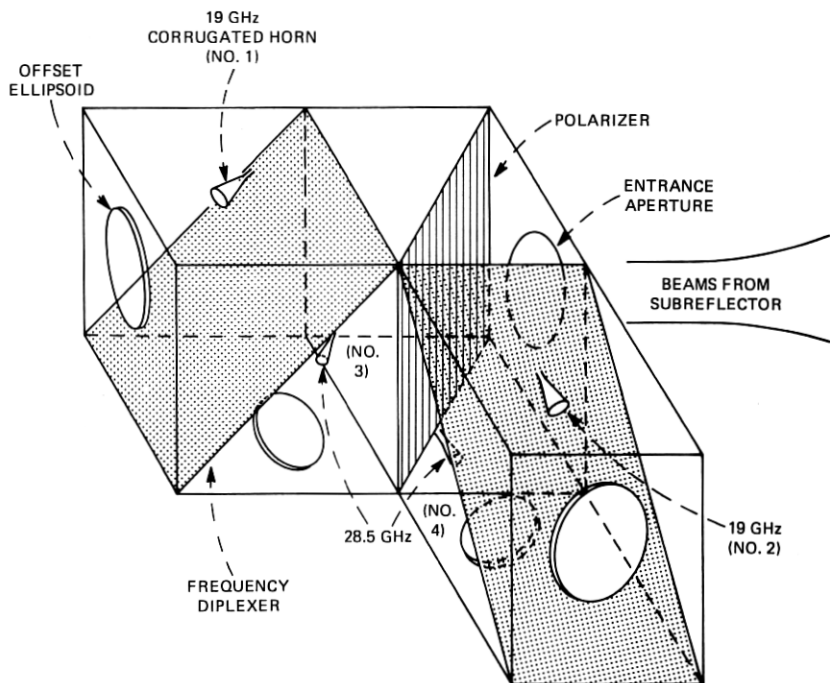
Fig. 3—Sketch of a 19/28.5 GHz dual-polarization feed system. The beam from the subreflector passing through the entrance aperture is first split by the polarizer and then subdivided by two frequency diplexers.

receivers. This feed system was first tested on axis, but operates in a position to produce a beam 0.5 degrees off-axis in azimuth, leaving the on-axis feed position free for the higher frequency radio astronomy feed. This off-axis operation results in very little degradation in the antenna pattern.

Past experience has shown that, after aging, radome surfaces hold thick water films during rain, causing large microwave attenuation.[10] The 7-m antenna was therefore designed without a radome, but with thermal insulation of critical parts of the structure to allow operation in the sun without significant degradation of pointing or surface accuracy. The support structure affords stiffness sufficient for operation at 30 GHz in winds up to 70 mph.

2.2 Mechanical description

The mount for the 7-m antenna is a conventional elevation-over-azimuth design with a single 2-m diameter cross-roller azimuth bearing and a yoke holding the elevation bearings. The elevation moving structure is built around a steel box girder. One end of the girder has a 32-cm bore

spherical roller bearing. The other end has a 1.4-m bore radial roller bearing sized to provide a 1.2-m diameter path to the side cab from the vertex area. The surface of the box girder facing the subreflector has a 1.6-m opening for the RF beam, completing the path from the subreflector to the elevation axis. A truss girder above the box girder supports the nine steel trusses that are radial to the axis of the main reflector and support its surface panels. The center truss is the longest and has been made deeper than the others by connecting its outer member to the elevation wheel support structure. The stiffness of the other trusses was adjusted using computer calculations so that gravity and wind deflections are expected to introduce mainly pointing errors with only small deviations of the antenna surface from its parabolic shape.

The 27 surface panels are arranged in four approximately equal width rings. The panels are A356 aluminum castings containing 17-cm deep ribs on the back side near the edges. These are joined by 9-cm deep ribs running in the circumferential direction with spacings of approximately 30 cm. The castings were tempered to T51, rough machined on a numerically controlled milling machine, stress relieved, and then machined to the final contour on the same machine. The manufacturer tested all the panels on his milling machines and found the surfaces to be accurate to better than 50-μm rms with an average value of about 40 μm. One of the early panels was tested on a Portage measuring machine and was found to have the same rms error (37 μm) as determined by the manufacturer. It was then subjected to 10 rapid temperature cycles from $-40°C$ to $60°C$ and back. Remeasurement on the Portage machine showed that the surface error had increased to 50-μm rms.

After machining, the panels were cleaned and painted with a 30 to 50-μm coat of an Alkyd base, TiO_2 pigment, flat white paint. After final alignment of the panel corners to the alignment template (see below), five panels near the center were measured against the template on an 18-cm grid. One of these panels was found to have a much larger surface error (100-μm rms) than expected with one bad area and a general warp. A visual inspection showed this bad area to be by far the worst on the antenna. However, it is only a small contribution to the total surface error of 100-μm rms.

The panels are held to the back-up structure by 2.54-cm diameter adjusting bolts. At the panel end, these bolts attach to machined pads in the corners of the peripheral ribs with ball and socket joints to avoid transmitting torques to the panels. These adjusting bolts are perpendicular to the surface and bend to take up the differential expansion between the aluminum panels and the steel backup structure.

Alignment of the surface panels was accomplished using a sweep template (Fig. 4) for reference. This was done under a tent with the antenna in the vertical look position, before installing the subreflector
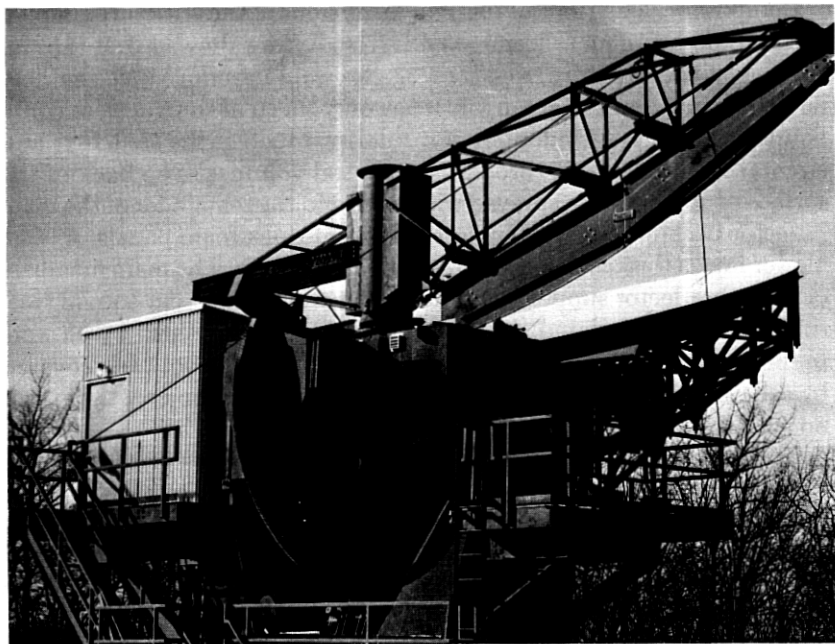
Fig. 4—Panel alignment template mounted in place of subreflector support tower above 7-meter reflector prior to installation of tent. The template consists of two sections joined by a link.

support tower and the vertex equipment room. The alignment template was machined in two parts, each of which has a reference hole at each end. The reference holes at the outer end of the inner template and the inner end of the outer template are at the same height and were joined by an accurate link. A counterweighted boom built on an adjustable vertical bearing supported the template. Another link adjusted the inner hole of the inner template to the correct radius from the rotational axis. Before each use, the vertical axis was set using an electronic tiltmeter, and the four template reference holes were set to their required relative height using gravity-oriented links on an optical level. Twelve transducers were attached to the template at radii corresponding to the panel mounting screws. They were referred to the accurate bottom surface of the template and used to measure panel corner positions.

The subreflector support structure has been kept well below the axis of the main reflector, especially near the secondary focus. This, coupled with the oversized subreflector, allow beams up to 2 degrees off axis in azimuth or 1 degree in elevation to be launched from the vertex equipment room. The subreflector itself is a machined aluminum casting of the same material and temper as the panels. It was machined on a vertical lathe and has a measured surface accuracy of 20-μm rms.

Computer calculations of thermal distortions of the structure coupled with temperature measurements on a test fixture showed that the sun shining on the structure from some angles would produce unacceptably large pointing and surface errors if the only thermal control were white paint. A strategy was adopted of insulating much of the structure and circulating ambient air through the critical volumes. The back of the surface panels has been sprayed with foam and the remainder of the main reflector backup structure enclosed by 5-cm-thick foam panels. A large blower floods this insulated volume with ambient air. The main members of the subreflector support structure are made of 10.16-cm-square steel tubing and are insulated. Ambient air is blown along them by blowers in the elevation girder. Most of the remaining steel structure is covered by 5-cm-thick panels of foam to increase thermal time constants, but no air circulation is provided.

In addition to shielding the backup structure from solar heat, the insulation of the back of the main reflector surface panels reduces the heat flux through the panels and hence the steady-state temperature difference between their surface and ribs. The penalty, however, is an increase (~2X) in the temperature rise of the surface panels in the full sun. This uniform temperature rise has the same effect as an absolute temperature change on the differential thermal expansion between the steel backup structure and the aluminum panels. It causes the panels to expand or contract in a direction parallel to the surface of the paraboloid defined by the backup structure. This has an almost negligible effect on the performance of the antenna. Warping of the panels due to thermal gradients perpendicular to their surface or thermal warping of the backup structure is much more important.

Two equipment rooms are on the antenna structure (Fig. 1). The vertex equipment room and the hollow elevation girder behind it provides a mounting space for receivers at the Cassegrainian focus. They move in elevation angle with the antenna. A double window of 50-μm Mylar* sheet allows RF energy to pass into this area with negligible loss (~0.1 dB) at 100 GHz. The side cab is provided for the Nesmyth focus. It moves only in azimuth. At present, it contains only receiver support equipment and the main elevation cable wrap. An 8-m by 6-m control building 15 meters from the antenna contains the rest of the receivers, the control computer, and a work area.

The volume under the azimuth bearing contains the azimuth cable wraps. A maypole wrap is used for most of the cables, but an auxiliary clock spring wrap carries the phase-sensitive RF cables.

The drive for each axis uses a single bull gear with two motors connected to separate speed reducers and pinions. The amplifiers for the two motors are biased so that, for low torque output, they torque in op-

---

* Registered trademark of E. I. Dupont.

posite directions to eliminate backlash, but when more than 15 percent of the maximum torque is required the opposing motor reverses. Each of the four dc motors is rated at 3 horsepower with phase control excitation. The gearing is chosen to give a slew speed of 1 degree/s in elevation and 2 degree/s in azimuth with 1 degree/s^2 acceleration in both axes and the ability to hold position or drive to the stow position in a 70-mph wind. This gearing results in the motor inertia dominating the antenna's inertia. Each motor has a brake with the same torque rating as the motor. When the drive system returns to standby from an active condition, the brakes are set before the motors relax so that the anti-backlash preload of the gear system is maintained.

The analog portion of the drive system is set up as a velocity control loop. Each drive motor has a tachometer generator. The sum of the tachometer signals is used in the main feedback loop, and the difference is used to damp possible oscillations in which the motors move in opposite directions.

Each axis has a direct drive Inductosyn* system which has an angular accuracy of 0.001 degree and a resolution of 21 bits. The antenna's minicomputer reads the position of each axis every 10 ms, subtracts it from the desired position, and applies the scaled difference to the drive system as a velocity command. Drive system overshoots are minimized by compressing the gain of the feedback loop within the computer by a factor of 4 for command velocities greater than $1/4$ of the maximum velocity. This strategy keeps the commanded velocity below the deceleration limit of the drive system when approaching the final position. When a source is tracked that moves at the sidereal rate or slower, the servo error has not been observed to exceed 0.001 degree with winds up to approximately 50 mph.

III. 19/28.5 GHz DUAL POLARIZATION FEED SYSTEM

3.1 Quasi-optical diplexers

The polarization diplexer (see Fig. 2) is simply a polarization grid made by photo-etching a copper-covered Mylar sheet. Copper strips 0.25-mm wide and 0.018-mm thick are spaced 0.25-mm apart on a Mylar sheet 0.013-mm thick. The grid is mounted on an aluminum supporting frame with an oval-shaped aperture of 33.02 cm by 48.26 cm. To achieve a flat grid, the supporting frame is made of jig plate instead of regular aluminum stock, which shows warping after machining. The plane of the grid is oriented at 45 degrees with respect to the incident beam from the subreflector. The conducting copper strips are perpendicular to the plane of incidence to avoid cross-polarized radiation[9] for both transmitting and reflecting orthogonal polarizations being diplexed.

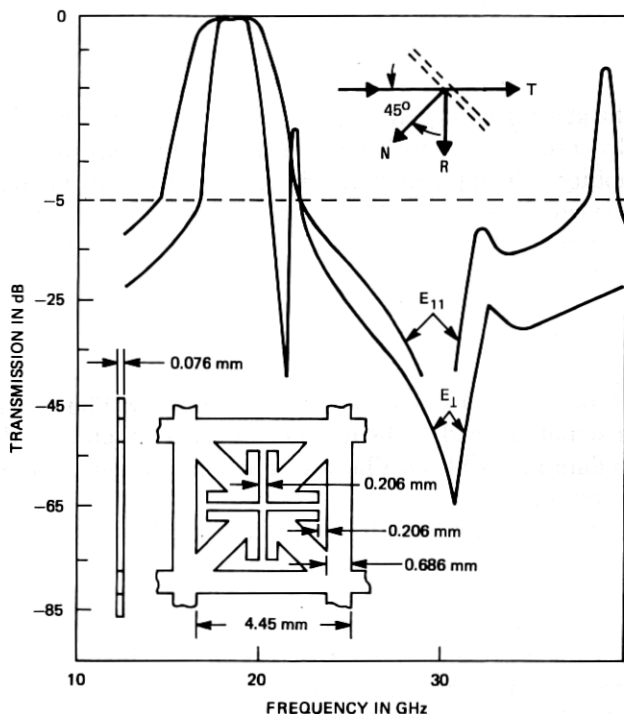* Registered trademark of Farrand Industries, Inc.

Fig. 5—Transmission of a double-self-supported frequency diplexer (see Fig. 3) with the indicated dimensions of the grid mask at 6.3 mm spacing and 45-degree angle of incidence for two polarizations.

Each of the two frequency diplexers is a pair of self-supported grids made of beryllium copper 75-μm thick. The 6.3-mm spacing between the girds is maintained by mounting on opposite sides of an aluminum frame with an oval aperture of 30.5 cm by 45.7 cm. Figure 2 shows that the polarization for Feeds No. 1 and No. 3 is perpendicular to the plane of incidence at the frequency diplexer, while that for Feeds No. 2 and No. 4 is parallel to the plane of incidence. The transmission characteristics for both polarizations and the dimensions of this double-self-supported grid are given in Fig. 5, which has been taken from Arnaud and Pelow's article.[8] The measured insertion losses for both transmitting 19.04 GHz and reflecting 28.56 GHz are less than 0.1 dB. Figure 5 also shows essentially perfect transmission and rejection frequency bands of well over 2 GHz each. This performance should be compared with a minimum insertion loss of 0.2 dB and a 2-GHz band loss of up to 1 dB for a typical waveguide diplexer at 19 and 30 GHz.

Several alternate quasi-optical frequency diplexers were tested. For a large (45-degree) angle of incidence, none of them achieved the desired transmission (−0.1 dB) and rejection (−20 dB) simultaneously for fre-
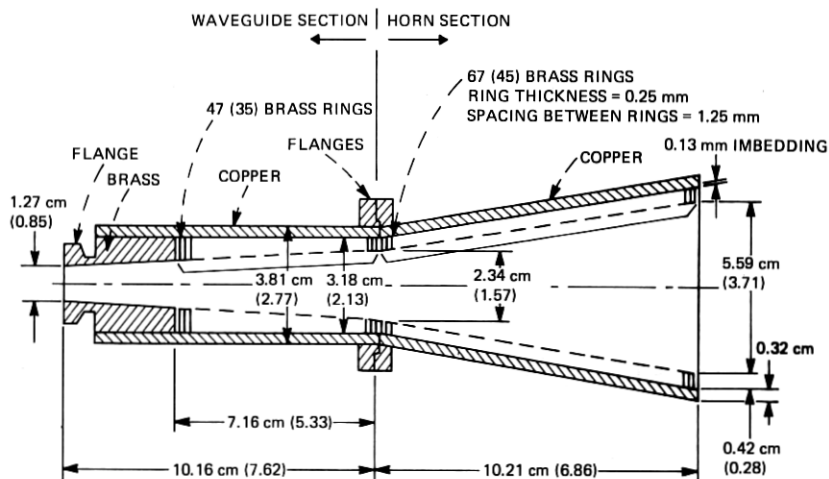
Fig. 6—The 19(28.5)-GHz conical corrugated horn and its hybrid mode launcher.

quency bands in the ratio of 1.5 to 1. A single gridded Jerusalem-cross diplexer[8] showed a transmission loss of 0.2 dB at 19 GHz for the polarization perpendicular to the plane of incidence and a rejection of only −10 dB at 28 GHz for the polarization parallel to the plane of incidence. When Mylar substrates were added to the double self-supported grid for improving its mechanical strength, transmission losses of 0.4 and 0.2 dB were observed at 19 GHz for the perpendicular and parallel polarizations.

The mechanical resonance frequency of the quasi-optical grids has been measured to be around 80 Hz, which is well above the passband of the baseband data in the COMSTAR beacon experiment.

3.2 Corrugated horns

Four corrugated horns (two each at 19 and 28.5 GHz) were constructed to illuminate the offset elliposids. The dimensions of the 19-GHz corrugated horn are illustrated in Fig. 6, where the numbers inside the parentheses are essentially scaled designs for 28.5 GHz. They are shortened versions of a very long corrugated horn built by Dragone.[11] The impedance matching between the smooth wall of the circular waveguide and the quarter wavelength slots of the corrugated horn is provided by a linear taper from half-wavelength corrugations that behave like a conducting surface. The 19-GHz transition from 1.27-cm diameter circular waveguide to 1.067 cm by 0.432 cm rectangular waveguide is hardware from the DR-18A terrestrial 18-GHz digital radio system. This transition consists of a tapered section from circular to square shape and a quarter-wavelength transformer. The 28.5-GHz transition from
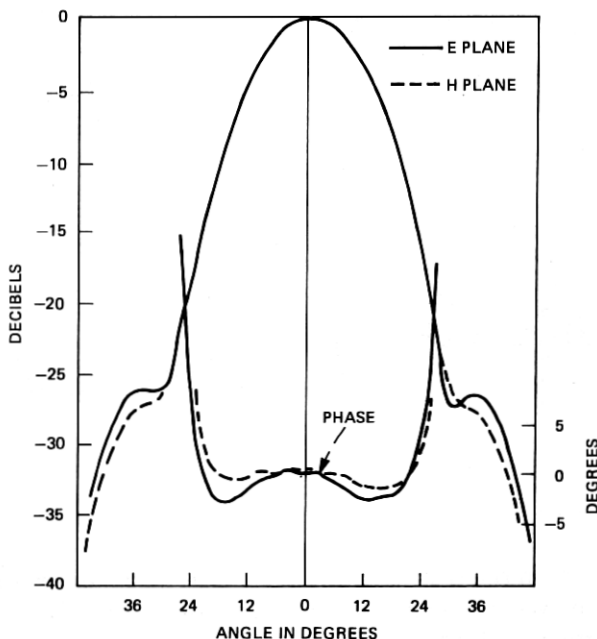
Fig. 7—Measured radiation patterns of 28.5-GHz corrugated horn. Rotation center 1.42 cm behind horn aperture.

0.846-cm diameter circular waveguide to 0.711 cm by 0.356 cm rectangular waveguide was also similarly designed. The measured return loss of all horns is better than 35 dB at the beacon frequencies 19 GHz and 28.5 GHz, and remains better than 31 dB over a 2-GHz band.

The measured far-field radiation patterns of the corrugated horns are shown for 28.5 GHz in Fig. 7, which are in excellent agreement with the calculations. The measured patterns at 19 GHz are essentially the same as those in Fig. 7, with the phase center located at 2.13 cm behind the horn aperture. The offset ellipsoid intercepts the horn radiation in the Fresnel region. It is difficult to measure the radiation pattern at a distance corresponding to the ellipsoid location. However, the calculated 20-dB half-beamwidth of the Fresnel zone radiation pattern is 2 degrees broader than those of the far-field patterns, and will be the same as the 28-degree half-cone angle of the ellipsoid subtended at the focus as shown in Fig. 8.

3.3 Offset ellipsoids

To be mirror-imaged at the Cassegrainian focal region (secondary geometrical focus of the subreflector for the on-axis case), the common phase center of the four offset launchers should be located in the middle
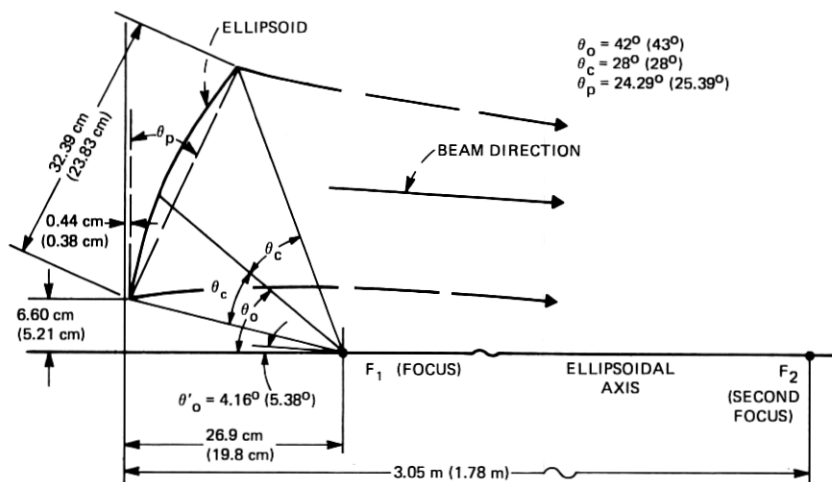
Fig. 8—Schematic diagram of the 19(28.5)-GHz offset ellipsoid.

of the feed box as shown in Fig. 9. Therefore, ellipsoids instead of paraboloids were used in the design of the feed system. One notes that a small movement of the phase center can be accomplished by the defocusing of a paraboloid. However, to place the phase center at a considerable distance in front of or behind a reflector with a small F/D ratio, an ellipsoid or a hyperboloid should be used. The design of an offset launcher
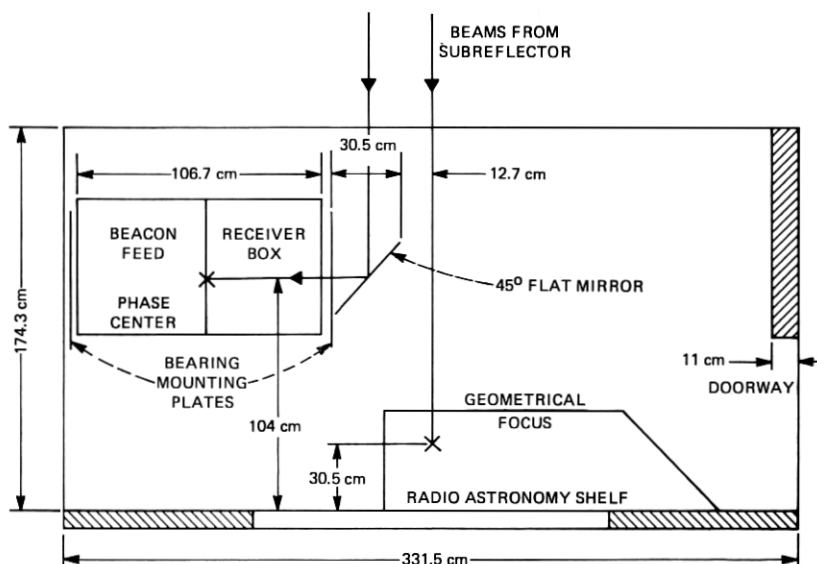

Fig. 9—Top view of vertex equipment room which has a height of 2.3 m and moves with the antenna.

was started with estimates by Gaussian beam approximation[12–14] and finalized by computer simulations which were essentially numerical integration of diffraction integrals,[2,15] assuming various design parameters.

Dimensions of both 19-GHz and 28.5-GHz offset ellipsoidal launchers are given in Fig. 8. Since the distance between the phase center and the 28.5-GHz elliposid is much greater in wavelengths than that of 19 GHz, the 28.5-GHz ellipsoid has larger size and greater curvature than a scaled version of the 19-GHz ellipsoid. The offset ellipsoid is subtended by a circular cone at the focus. The offset angle of the feedhorn axis is 3 degrees greater than that of the cone axis; thus approximately equal illumination taper can be achieved on the top and bottom edges of the reflector. The intersection of an ellipsoid and a circular cone subtended at one focus is a plane ellipse subtended by another circular cone at the other focus. The radiating beam from the ellipsoid will lie along the latter cone axis which deviates from the major axis of the ellipse by 4.16 degrees at 19 GHz and 5.28 degrees at 28.5 GHz. Aluminum jig plates 2.54-cm thick are first cut into ellipses of 32.41 by 30.43 cm and 23.85 by 22.40 cm; then they are positioned and oriented correctly with respect to ellipsoidal axes for computer-controlled numerical machining.

3.4 Mechanical mounting

All the components are mounted in an L-shape frame of 106.7 × 106.7 × 61 cm as illustrated schematically in Fig. 2. The frame is made of structural aluminum angles with sufficient diagonal bracing to insure rigidity without blocking the radiating beams. The mounting of corrugated horns and offset ellipsoids was designed to allow adjustment for positioning, orientation, and focusing.

Owing to the uncertainty of the orbital position assignment for the COMSTAR satellite, the polarizations of the beacon signals were not precisely given. Therefore physical rotation of the feed frame around the beam axis is needed to match an arbitrary pair of orthogonal linear polarizations.* This required rotation is accomplished by a thrust ball bearing with 33-cm diameter circular opening in the front and a floating bearing in the back. These bearings are mounted on an aluminum supporting frame as shown in Fig. 10. This bearing mount is directly attached to steel I-beams through holes in the floor of the vertex equipment room of the 7-m antenna. The connection between the bearing mount and the steel I-beam allows differential thermal expansion between the indoor aluminum structure and the outdoor steel structure.

---

* This rotation is also needed for calibrating the amplitude and phases of the cross-polarized signals received from the satellite beacons.
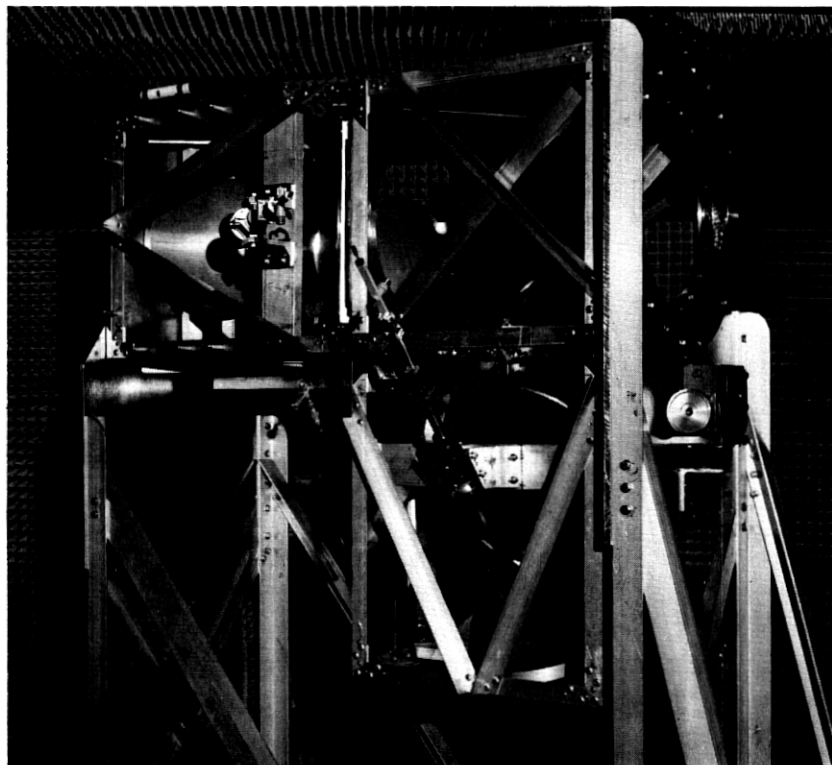
Fig. 10—A 19/28.5 GHz duo-polarization quasi-optical feed system (see Fig. 3) for the beacon measurements.

The 45-degree flat mirror, which consists of a 0.794-cm-thick aluminum jig plate, is mounted in front of the 33-cm bearing opening as shown in Fig. 9. Both azimuth and elevation orientations of the mirror can be adjusted around its center to facilitate experimental search for proper illumination of the subreflector. An oversized mirror of 38.10 by 53.34 cm oval shape was used in the initial measurents of the 7-m antenna. However, a smaller mirror of 30.48 by 43.18 cm shows very little truncation effect and is used in the beacon propagation experiment.

3.5 Measured results of the feed system

The design objective of the feed system is for each of the four offset launchers to illuminate the subreflector with a spherical wave of 15 dB taper over a 10-degree sector from a common phase center, with very low cross-polarized radiation as well as very low insertion loss of the quasi-optical diplexers. To achieve and demonstrate the desired performance, we aligned the components through pattern measurements in an ane-
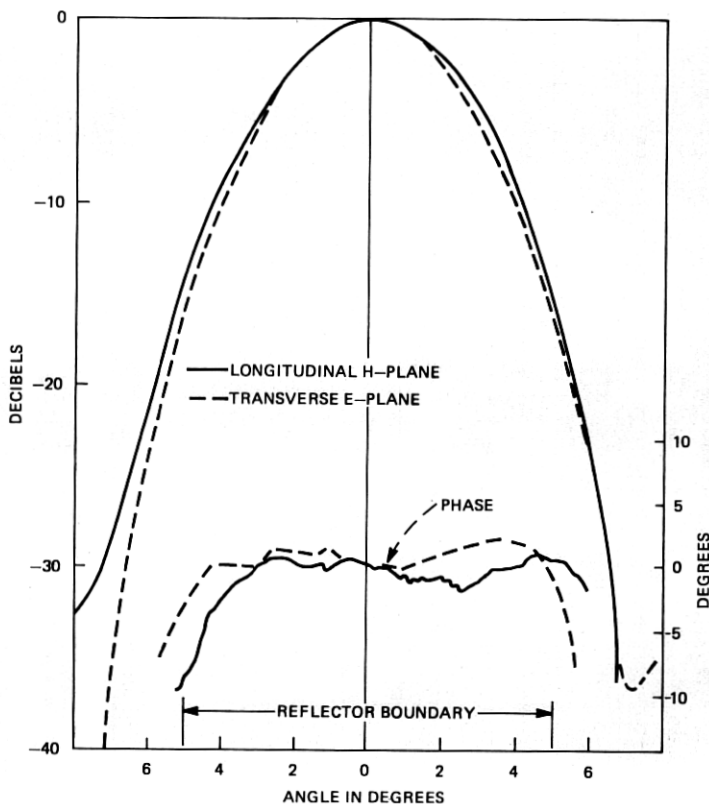
Fig. 11a—Measured radiation patterns of Feed No. 1 at 19 GHz (see Fig. 3).

choic chamber. To simulate the illumination of the 7-m offset Cassegrain antenna, the distance between the transmitting source horn used in the pattern measurements and the phase center of the receiving feed system was the same (526 cm) as that between the subreflector and its geometrical focus. Mechanical alignment was established before electrical measurements.

The measured insertion loss for a quasi-optical polarization or frequency diplexer was found to be 0.1 dB or less in each case. Amplitude and phase patterns were measured with respect to the common rotation center and the common optical boresight. After a few iterative adjustments of orientations and locations for both corrugated horn and ellipsoid, good agreement between measured and calculated patterns was achieved for each offset launcher. In particular, the measured patterns verified the calculated beamwidth, the effective phase center of the offset ellipsoids, and the approximate pattern symmetry predicted in the asymmetrical offset plane.
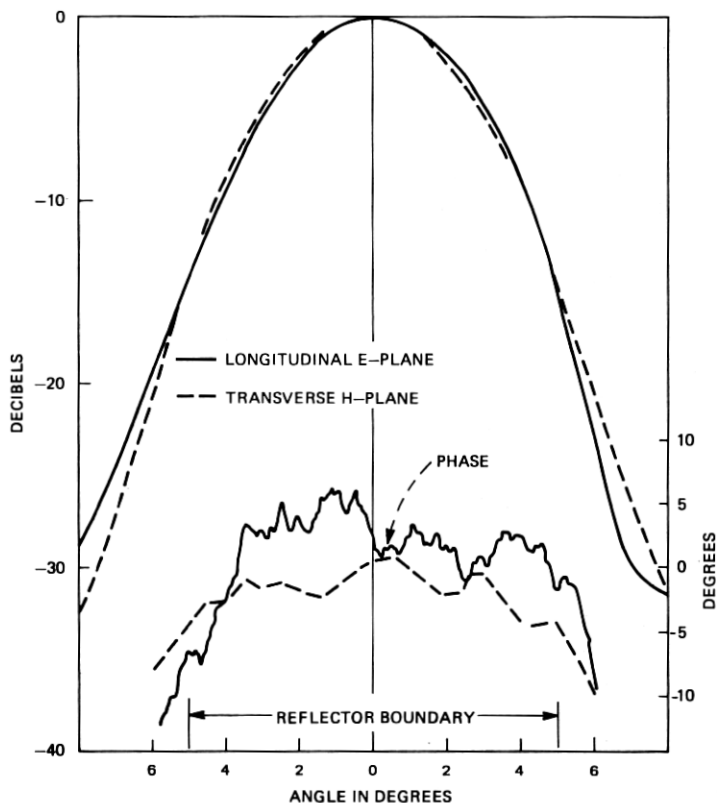
Fig. 11b—Measured radiation patterns of Feed No. 3 at 28.5 GHz (see Fig. 3).

The final measured patterns of Feeds No. 1 (19 GHz) and No. 3 (28.5 GHz) are shown in Fig. 11 for both E and H planes. Essentially identical measured patterns were obtained for the orthogonally polarized pair of Feeds No. 2 (19 GHz) and No. 4 (28.5 GHz). Following the nomenclatures used for horn reflector antennas, the longitudinal plane is the asymmetrical offset plane which divides the ellipsoid into two symmetrical halves and the transverse plane is the orthogonal principal plane. The measured phase patterns are less than ±5 degrees from a common spherical phase front while the measured amplitude patterns are within ±0.5 dB of perfect coincidence over the 15-dB pattern-width illuminating a 10-degree sector with respect to the common boresight. The cross-polarized radiation remained below −45 dB for all directions. It was found necessary to cover both the transmitting horn and the front bearing mount of the receiving feed system with absorbers to avoid excessive interactions. The ripples in the measured phase patterns of Fig. 11 were identified as the effects of the residual interactions.

The measured phase patterns of Fig. 11 imply an alignment accuracy of about $\frac{1}{100}$ beamwidth among the beams for the beacon receiver of the 7-m antenna. One notes that any moderate asymmetry or misalignment of the amplitude pattern of the feed system, which has little effect on the beam-pointing accuracy, can be tolerated in a communication system. However, good alignment of the feed amplitude patterns is essential to the stability of the differential phase between the beams of the 7-m antenna.

After the alignment measurements, the RF stages of the receiver[16] for the 19- and 28.5-GHz beacon experiment were mounted on the feed frame. The alignment was then checked using the beacon receiving system. Tests were made on the thermal stability of the differential phase between the two orthogonally polarized 19-GHz feeds. The change of the differential phase with respect to temperature was about 0.1 degree per 1°F and could be partially explained by the difference in waveguide lengths. Local heating of the polarization-diplexing grid shows a 0.2-degree change of the differential phase.

Since the calibration of the beacon receiver makes use of the rotation of the feed frame around the beam axis, the behavior of the differential phase during this rotation was examined. When the two orthogonal linearly polarized incident waves are of comparable magnitude (i.e., when the transmitting polarization is oriented at roughly 45 degrees with respect to the orthogonal polarizations of two 19-GHz receiving feeds), the measured differential phase remains essentially constant (within 0.1 degree) over a 10-degree rotation of the feed frame around the beam axis. When the two orthogonal linear polarizations are of vastly different magnitude, the measured differential phase can involve a substantial error because of a phase quadrature component arising from cross-polarization coupling. Even a polarization grid cannot effectively discriminate against an incident cross polarization of a magnitude much greater than that of the in-line polarization.

IV. MEASUREMENTS OF THE 7-METER ANTENNA

4.1 Transmitting sources

To measure the gain and radiation patterns of the Crawford Hill 7-m antenna, a weatherproof box, which contains transmitting sources at 19, 28.5, and 99.5 GHz was placed on an AT&T Long Lines tower at Sayreville, N.J., approximately 11 km from Crawford Hill. Two horn-lens antennas with polarization grids (providing cross-polarization discrimination better than 50 dB) are used for vertical and horizontal polarizations at the lower frequencies. Each antenna has a frequency diplexer and can transmit 19 and 28.5 GHz. Waveguide switches independently control the polarization or turn off each transmitter. The
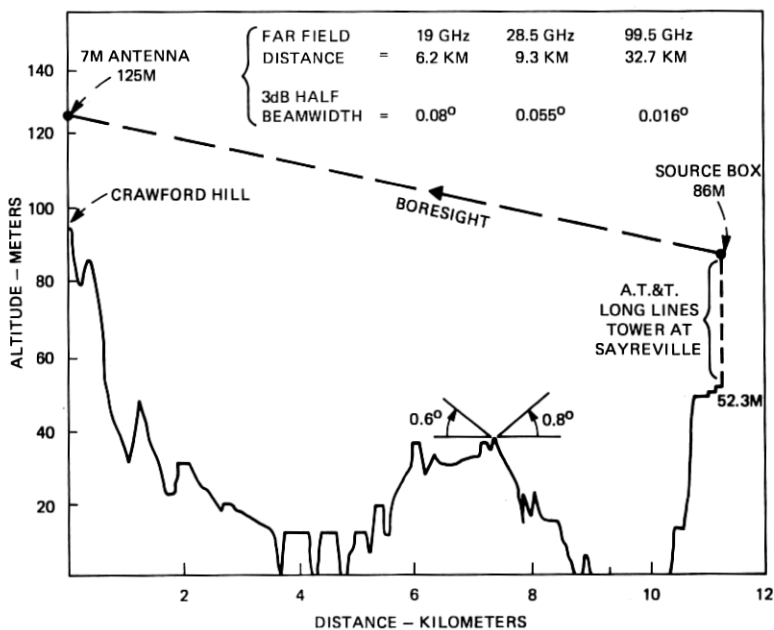
Fig. 12—Terrain profile of boresight range for 7-meter antenna.

antenna gains are 30 and 33 dB with half-power beamwidths of 6.5 and 5 degrees at 19 and 28.5 GHz, respectively. The sources at 19.04 and 28.56 GHz are 100-mw Gunn oscillators.

An antenna consisting of two cylindrical reflectors[17] with a dual-mode feed and a vertically polarized grid is used to transmit a 99.5-GHz signal from a 10-mw IMPATT source with only about 50-KHz FM noise. The oscillator is connected through an isolator directly to the feed horn. The antenna has a gain of 41.5 dB with a half-power beamwidth of 1 degree in the elevation plane.

Because of the distant location, the source box is remotely controlled from Crawford Hill. The beams from three source antennas were initially co-aligned before installation on the Sayreville tower. The expected power received by the 7-m antenna was about −30 dBm at all three frequencies.

4.2 Probing measurements of the incident field

In evaluating measured results of a large aperture antenna, it is necessary to know the field distribution incident on the aperture from a distant transmitting source. The path profile of the Sayreville to Crawford Hill measuring range is shown in Fig. 12. Although the well-elevated transmitting and receiving sites provide a clear line of sight,
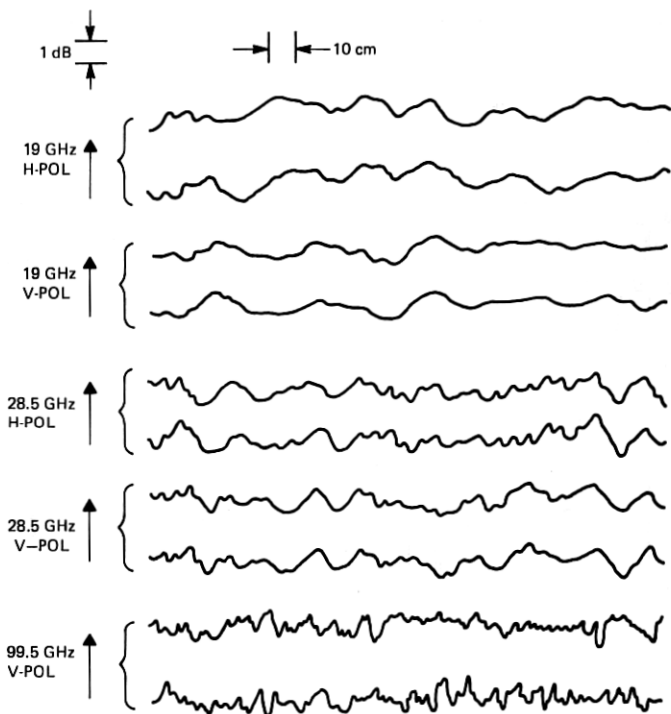
7-METER MILLIMETER WAVE ANTENNA   **1275**

Fig. 13—Sample vertical scans for each of the five transmissions from source at Sayreville. Repeatable scans at 19 and 28.5 GHz indicate small reflections from the terrain. Uncorrelated scans at 99.5 GHz indicate atmospheric scintillations.

there still exist potential reflectors and scatterers of the millimeter-wave energy transmitted from Sayreville. A carriage and radial track mechanism was designed to permit a probe antenna to be moved along a diameter of a circular aperture to obtain field amplitude measurements. The incident field along four diameters of the 7-m aperture with 45-degree angular separation was scanned for each of the five possible states of transmission, i.e., vertical and horizontal polarizations at both 19 and 28.5 GHz and vertically polarized 99.5 GHz. Each scan was made twice to check on repeatability.

Figure 13 shows sample segments of scan pairs for all five transmissions. The good duplications of fluctuations at 19 and 28.5 GHz indicate that the systematic deviations in the field are results of specular reflections and diffractions. At 99.5 GHz, very little correlation exists between scans on a given diameter. Here the fluctuations are mostly atmospheric scintillations rather than terrain reflection. One notes that the 99.5-GHz transmitting antenna at Sayreville has a much narrower beamwidth than those of lower frequencies and the electrically rougher terrain is much less specular.

The spatial variations of the scan data suggest that most of the scattering comes at large angles with respect to the transmission path. This observation has been indeed confirmed by angular spectra obtained from a Fourier transform of the data. Hence, the terrain reflections should be negligible in the received power of the 7-m antenna pointing directly toward the transmitting source. The effect on the measured patterns will be only minor disturbance on sidelobes in the elevation plane at 19 and 28.5 GHz when the antenna is pointing below the source.

The received power in a gain-standard horn, which has a gain of the same order as that of our probe horn, will exhibit similar fluctuations across the aperture as those of Fig. 13. Since the fluctuations at 99.5 GHz are mostly atmospheric scintillations, the uncertainty arising from this fluctuation can be suppressed by taking an average of a number of comparisons between the gain standard and the 7-m antenna. However, at 19 and 28.5 GHz, the fluctuations are caused by terrain reflections; to reduce the uncertainty here, an average needs to be taken of numerous horn locations over the aperture. Analysis of the data resulting from probing measurements indicates that scanning the horn over a 1.4-m aperture segment gives a standard deviation of 0.4 dB at 19 GHz and 0.34 dB at 28.5 GHz.

4.3 Prime focus measurements

To provide an evaluation of surface tolerance as well as to locate the primary focal point of the 7-m reflector for subsequent installation of the subreflector, we first conducted 99.5-GHz prime focus measurements using a dual-mode feedhorn with 20-dB taper at the reflector boundary. The measured feed patterns are shown in Fig. 14. The focal region was probed with the feed until the best patterns were obtained. The measured patterns in the azimuth and elevation planes are shown in Fig. 15 together with the calculated pattern envelope assuming a perfect reflector surface.[2] The calculated patterns are approximately the same for azimuth and elevation. Expanded patterns not shown here indicated good agreement between measured and calculated half-power beamwidths (0.032 degree); however, the measured sidelobe levels are higher than the calculated values especially in the elevation plane. It is of interest to note that only near sidelobes in the elevation plane are higher than the corresponding lobes in the azimuth plane, whereas the far sidelobes in the two planes are essentially similar. Furthermore, the measured far sidelobe levels are consistent with an rms surface roughness of 0.1 mm. The excessive near sidelobe level in the elevation plane appears to be caused by a surface distortion of large-scale size. Since the reflector panels were set using a two-section template, a relative misalignment of these two sections could cause the elevation patterns we observed. This conjecture has been confirmed by pattern calculations
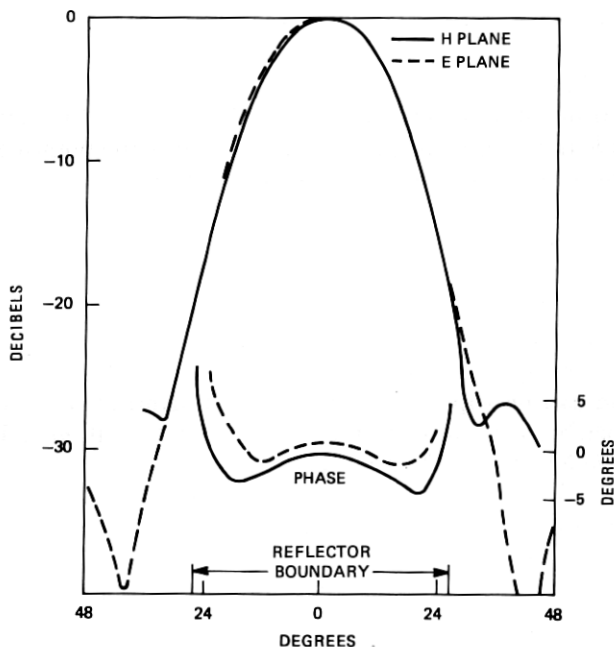
Fig. 14—Measured patterns of 99.5-GHz dual mode horn (0.98-cm diameter aperture) for prime-focus feed.

assuming a relative displacement (~0.15 mm) between two sections of the template.

Gain measurements of 99.5 GHz for the 7-m offset reflector using prime focus feed were made by comparison with a calibrated gain standard.[18] The comparisons were made at various times of day to obtain some estimate of the effects of scintillation. A time constant of about 1 s was used in the measuring set to smooth out the scintillation. Measurements indicate that gain variations due to diurnal variations of scintillations are generally less than about 0.2 dB. This observation has been also confirmed by the repeatability of measured patterns. A measured gain of 74.63 ± 0.45 dB was obtained from a sample of 10 comparisons with the gain standard taken on a clear quiet evening shortly after sunset.

The comparisons were made by measuring the difference in signal received by the gain standard (30.77 dB) and the 7-m antenna padded by a calibrated attenuator (40.05 dB). The error estimates of ±0.45 dB were obtained from the root-sum-square of the 3σ random errors: 0.14 dB for the calibrated attenuator, 0.16 dB for the gain standard, and 0.40 dB for the sample mean of 10 comparisons.

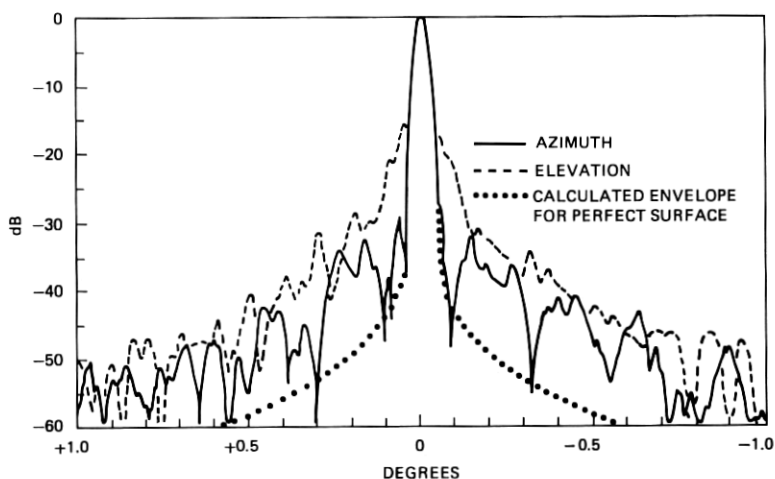The theoretical gain of the antenna at 99.5 GHz having no roughness

Fig. 15—99.5-GHz scan over a 2 degree range measured with prime-focus dual-mode feed of 20-dB taper. The difference between measured far sidelobe levels and the calculated pattern envelope for perfect surface is consistent[5] with 0.1 mm rms surface tolerance. The higher near-sidelobe level in the elevation plane stems from large-scale surface distortion.

is calculated as follows:

$$
\begin{aligned}
77.26 \text{ dB} &= \text{Area Gain} \\
-1.56 \text{ dB} &= \text{Illumination Taper} \\
-0.08 \text{ dB} &= \text{Spillover} \\
-0.2 \ \ \text{dB} &= \text{Feed Loss (Estimated)} \\
\hline
75.42 \text{ dB} &= \text{Calculated Gain for Perfect Surface}
\end{aligned}
$$

Using the formula $e^{-(4\pi\epsilon/\lambda)^2}$, where ϵ is the rms surface tolerance, we see the difference between measured and calculated gains, (0.79 ± 0.45) dB, corresponds to an rms roughness of (0.1 ± 0.03) mm.

Using a 20-dB taper corrugated horn (see Figs. 6 and 7) as a prime focus feed, we also measured the patterns of the 7-m offset reflector at 28.5 GHz as shown in Fig. 16. Excellent agreement between measured and calculated patterns were obtained in the azimuth plane. However, as with 99.5 GHz, there was a noticeable discrepancy between measured and calculated sidelobe levels in the elevation plane. The first sidelobe is −25 dB compared with −16 dB at 99.5 GHz.

The measured gain at 28.5 GHz was obtained by padding the 7-m reflector with a calibrated attenuator (39.93 ± 0.05) dB, and comparing with a calibrated gain standard (24.98 ± 0.08) dB.[18] Using 15 different locations for the gain standard, the measured gain was determined to be (64.7 ± 0.6) dB. The large 3σ error limit was the consequence of the data spread and is consistent with the results of the probing measurements. The expected prime focus gain at 28.5 GHz can be calculated as
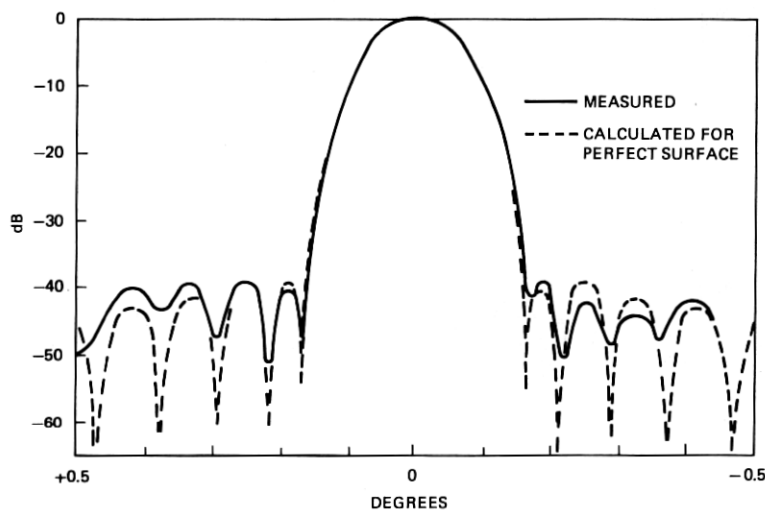
Fig. 16a—Measured 28.5-GHz azimuthal pattern with prime focus feed of 20-dB taper showing excellent agreement with calculated pattern for perfect surface.

follows:

$$\begin{aligned}
66.42 \text{ dB} &= \text{Area Gain} \\
-1.56 \text{ dB} &= \text{Illumination Taper} \\
-0.08 \text{ dB} &= \text{Spillover} \\
\underline{-0.1 \text{ dB}} &= \underline{\text{Feed Loss (Estimated)}} \\
64.68 \text{ dB} &= \text{Calculated Gain for Perfect Surface}
\end{aligned}$$

4.4 Subreflector alignment and measured results

The hyperboloidal subreflector is required to be confocal and coaxial with the paraboloidal main reflector. The primary focal point has been given by pattern measurements using prime focus feeds. Before installation of the subreflector, a laser beam was first fixed along the reflector axis. The subreflector was oriented with the aid of the laser beam reflected from a mirror attached to the bottom of the subreflector, centered on and perpendicular to its axis. The position of the subreflector was adjusted by interpreting the measured 99.5-GHz patterns until they were consistent with the prime-focus-fed patterns.

The Cassegrainian feed, used in the 99.05-GHz pattern measurements of the complete 7-m antenna including subreflector, consists of an offset ellipsoid and a dual-mode horn. The feed is essentially a scaled model of the 19-GHz offset launcher in the 19/28.5-GHz duo-polarization feed. Figure 17 shows that the measured 99.5-GHz feed patterns are almost the same as those of the 19/28.5-GHz feeds. Thus we can make direct comparison of measurements on the 7-m antenna at 99.5 GHz with the 19- and 28.5-GHz performance.
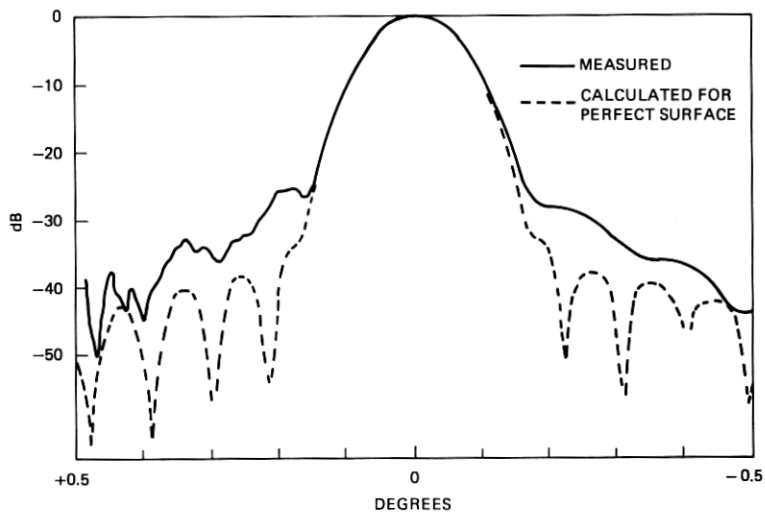
Fig. 16b—28.5-GHz elevation pattern with prime-focus feed of 20-dB taper. The measured first sidelobe level is −25 dB compared with −16 dB at 99.5 GHz in Fig. 15.
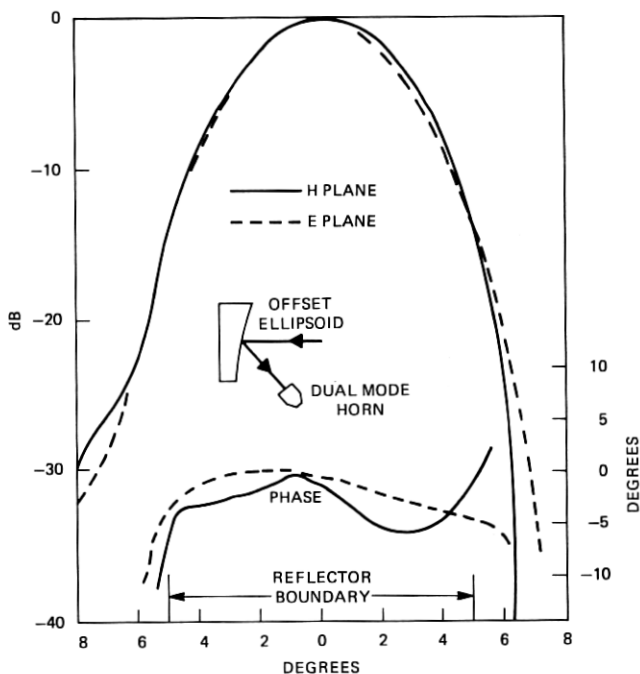

Fig. 17—Measured patterns of 99.5-GHz Cassegrainian feed consisting of an offset ellipsoid and a dual-mode horn.
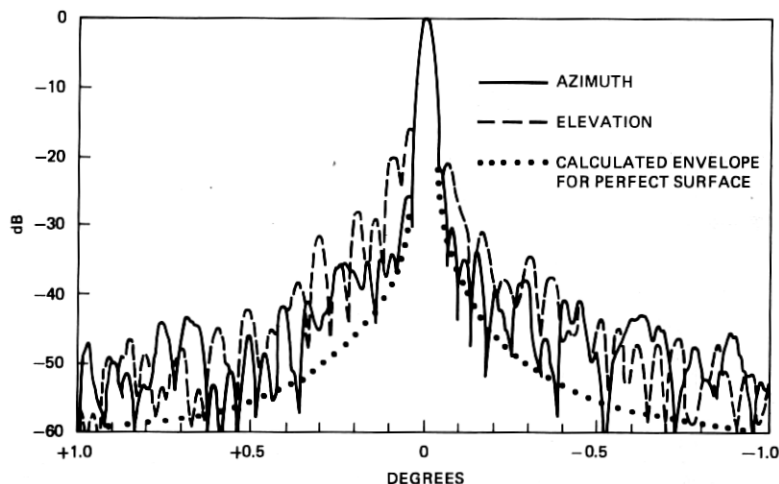
Fig. 18—99.5-GHz scan over a 2-degree range measured with Cassegrainian feed of 14-dB taper and compared with the calculated pattern envelope for perfect surface. The above patterns are consistent with those of prime-focus feed in Fig. 15.

Measured patterns are found to be insensitive to the location of the feed phase center as expected from the very long effective focal length of the antenna. With the feed phase center located on axis, the beam pointing of the Cassegrainian configuration agrees with that of the prime focus configuration to within 0.02 degree. Measured 99.5-GHz patterns are shown in Fig. 18 together with the calculated pattern envelope[15] for comparison. Measured half-power beamwidths agree with calculated values, whereas measured sidelobe levels are higher than calculated levels by about the same amount as in the prime focus measurements. Since the Cassegrainian feed has an illumination taper of 14 dB in contrast with the 20-dB taper of the prime focus feed, the sidelobe level is expected to be higher than that of the prime focus configuration. The measured first sidelobe level in the elevation plane is almost the same for prime focus and Cassegrainian configurations, because it is dominated by reflector distortion rather than illumination taper. It is seen that, as with the prime-focus case, the discrepancy between azimuth and elevation patterns is confined to the near sidelobe region, whereas the far sidelobe levels of two patterns merge together.

Pattern measurements were also taken for each of the four feeds in the duo-polarization 19/28.5-GHz quasi-optical feed assembly. The 7-m antenna was first tested with the 19/28.5-GHz feeds located at the on-axis position using both an oversized mirror of 38.10 by 53.34 cm oval shape and a smaller mirror of 30.48 by 43.18 cm. Measurements in each case showed the coincidence of four beam maxima for each polarization and frequency of the quasi-optical feed network. The smaller mirror
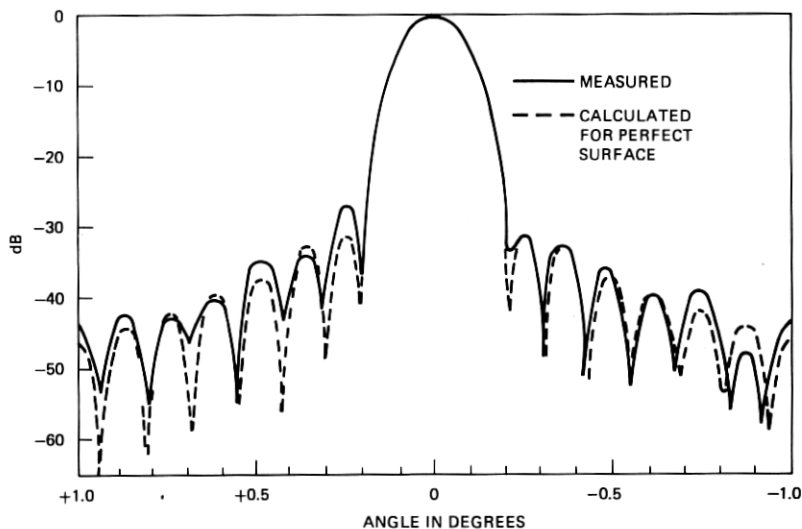
Fig. 19a—Measured 19-GHz azimuthal pattern with Cassegrainian feed of 15-dB taper and vertical polarization showing excellent agreement with the calculated pattern for perfect surface.

showed very little truncation effect in measured patterns. Following these on-axis measurements, the feed box for the beacon receiver together with the smaller mirror was moved to a position 0.5 degree off axis from the center of the vertex equipment room to allow clearance for an on-axis beam for millimeter-wave radio astronomy as shown in Fig. 9. As expected,[3,4] measurements showed very little difference between the 0.5-degree off-axis and on-axis beams for both 19 and 28.5 GHz.

Measured cross-polarized radiation for each on-axis beam remained below −40 dB in all directions with respect to the in-line polarization maximum, while that for each 0.5-degree off-axis beam is smaller than −39 dB. One notes that the optimum orientations of the polarization-grid diplexer for nulling the cross polarization are about 0.7 degree apart between two orthogonally polarized feeds. The above cross-polarization data were measured using a compromise orientation of the polarization grid.

Figures 19 and 20 show comparisons between measured and calculated patterns[15] at 19 and 28.5 GHz. The measured patterns were obtained from vertically polarized feeds at on-axis position with the smaller 45-degree mirror, and remained essentially the same for other combinations of polarization and mirror at both on-axis and 0.5-degree off-axis feed positions. Good match between calculated and measured azimuthal patterns is illustrated in Figs. 19(a) and 20(a), whereas the agreement between calculated and measured elevation patterns is, again, less sat-
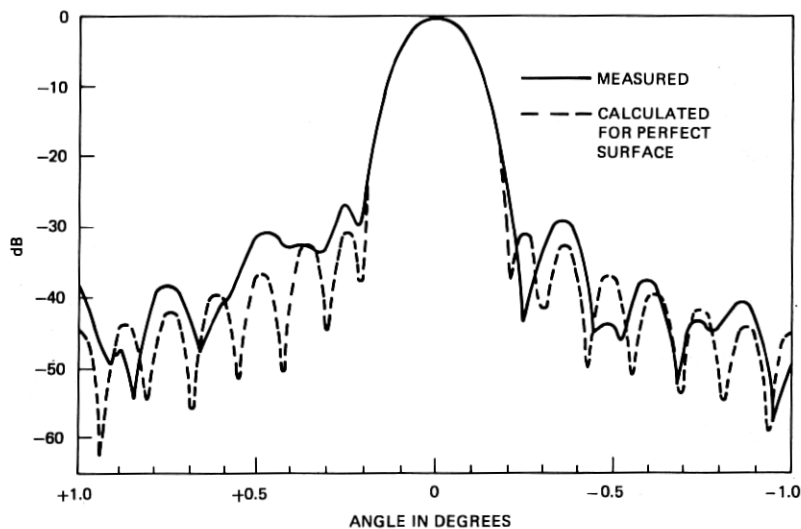
7-METER MILLIMETER WAVE ANTENNA   **1283**

Fig. 19b—Measured 19-GHz elevation pattern with Cassegrainian feed of 15-dB taper and vertical polarization showing fair agreement with the calculated pattern for perfect surface.

isfactory as shown in Figs. 19b and 20b. The measured sidelobes of all elevation patterns have generally shown, especially in Fig. 20b, a period twice that of the calculated value. This observation supports the conjecture about a relative misalignment of two sections of the template
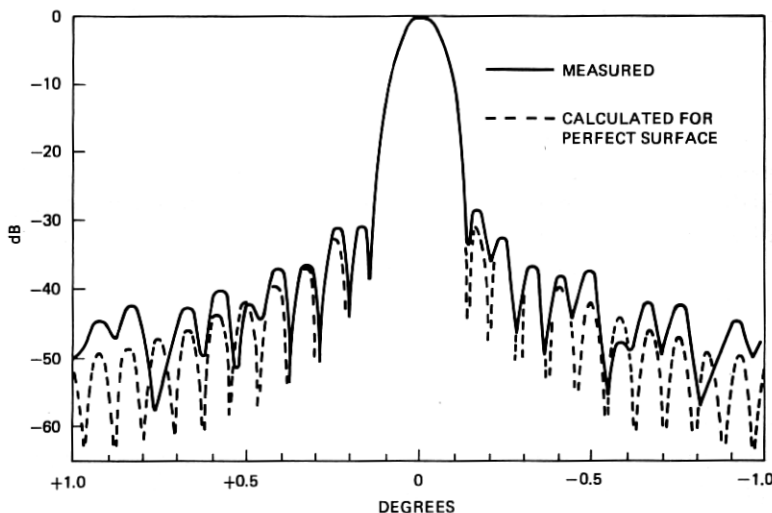

Fig. 20a—28.5-GHz azimuth pattern with Cassegrainian feed of 15 dB taper and vertical polarization. The measured pattern is consistent with that in Fig. 16a for prime focus feed of 20-dB taper.
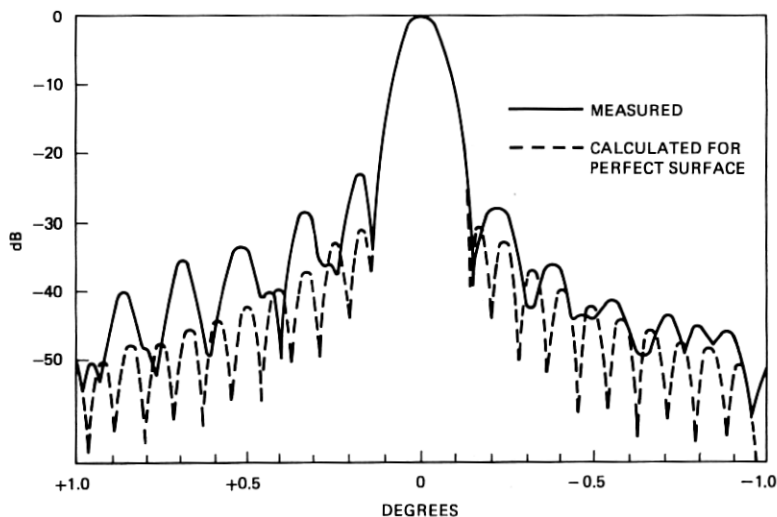
Fig. 20b—28.5-GHz elevation pattern with Cassegrainian feed of 15-dB taper and vertical polarization. The measured pattern is consistent with that in Fig. 16b for prime focus feed of 20-dB taper.

as discussed in Section 4.3. Measured 19-GHz sidelobe levels 1 degree away from the beam maximum are −43 dB in the azimuth plane and −38 dB in the elevation plane. These levels are of interest in avoiding interference from future adjacent satellites in synchronous orbits.

V. CONCLUDING REMARKS

The expected performance of the Crawford Hill 7-m antenna and its associated feed systems has been realized. This antenna is the first large offset Cassegrain in operation. Comparison between prime-focus-fed and Cassegrain-fed patterns shows very little degradation due to any surface imperfection or misalignment of the subreflector.

Comparison with a calibrated gain standard showed the difference between the 99.5-GHz measured and calculated prime-focus gains to be (0.79 ± 0.45) dB, which implies an rms surface error of about 0.1 mm. The measured 99.5-GHz azimuthal pattern appears to indicate a surface error of this magnitude, whereas the elevation pattern shows skewed shape and unexpectedly high near-in sidelobe level. Computer simulations have indicated that the distorted elevation pattern can be caused by a relative displacement (~0.15 mm) between two sections of the template used to calibrate the reflector panels. This explanation is also consistent with the measured gain because it is only accompanied by a small gain reduction (~0.15 dB).

Pattern measurements using the quasi-optical 19/28.5 GHz dual-polarization feed assembly have shown the coincidence of the four beams.

Table I — Derived Cassegrainian gain in decibels with 15-dB feed taper

Frequency (GHz)	99.5	28.5	19
Area Gain	77.26	66.4	62.88
Illumination Taper	−0.93	−0.93	−0.93
Spillover*	−0.35	−0.4	−0.45
Feed and Multiplexing†	−0.2	−0.2	−0.2
Surface Tolerance	−0.8	−0.1	−0.05
Derived Gain	74.98	64.77	61.25
Error Estimates	±0.5	±0.25	±0.25
Gain Efficiency	59.2%	68.7%	68.7%

* The estimates for spillover loss are higher at 19 and 28.5 GHz because of truncations in the quasi-optical 19/28.5 GHz duo-polarization feed.

† No multiplexing is involved at 99.5 GHz, whereas both frequency and polarization diplexing losses are included in the estimates at 19 and 28.5 GHz.

Cross-polarized radiation is −40 dB or less in all directions throughout each beam. The measured results have now confirmed the theoretical prediction[2] that there should be very little cross-polarized radiation from an offset Cassegrainian antenna with a large effective F/D ratio if the feed radiation is free of cross polarization.

Good agreement between calculated and measured patterns is shown in the azimuthal plane, whereas the comparison is less satisfactory in the elevation plane. At 1 degree away from the beam maximum, the 19-GHz sidelobe level is −43 dB in the azimuth plane and −38 dB in the elevation plane. Since the synchronous orbit is seldom close to the elevation plane of a ground station antenna, these measured sidelobe levels have practically achieved the objective of 40-dB discrimination between adjacent synchronous satellites at 1-degree spacing.

The gain measurement of the Cassegrainian configuration is hampered by the sensitivity of the harmonic mixer to the temperature difference between indoor and outdoor environments and by a lot of cable movement in addition to the terrain reflection problem at 19 and 28.5 GHz. However, having determined the main reflector surface tolerance by prime focus measurements, we can derive the Cassegrainian gains as shown in Table I.

Multiple-beam operation has been achieved with a 0.5-degree off-axis beam for beacon feed and an on-axis beam for millimeter-wave radio astronomy. Measurements showed very little difference between 0.5-degree off-axis and on-axis beams at both 19 and 28.5 GHz.

VI. ACKNOWLEDGMENTS

problems, including the main structure, subreflector, and feed system. M. J. Gans designed the vertex room windows and calculated the surface distortions from mechanical measurements. H. H. Hoffman collaborated on the antenna-receiver interface. D. C. Hogg proposed the antenna configuration. E. A. Ohm recognized the large beam scanning capability of the antenna configuration and modified the vertex equipment room and subreflector support structure design to facilitate launching beams at large off-axis angles while keeping the gravitational pointing error small. He also designed and supervised the fabrication of the subreflector. F. A. Pelow supplied the quasi-optical diplexers. A. Quigley and members of the shop built most of the feed hardware. H. E. Rowe examined detailed surface tolerance effects. J. Ruscio and T. Fitch took care of receiver cables in the cable wraps. R. A. Semplak provided the 99.5-GHz Cassegrainian feed. R. H. Turrin designed the carriage and radial track mechanism for probing measurements. D. Vitello programmed the pattern calculations. G. V. Whyte implemented the subreflector mount.

REFERENCES

1. C. Dragone and D. C. Hogg, "The Radiation Pattern and Impedance of Offset and Symmetrical Near-Field Cassegrainian and Gregorian Antennas," IEEE Transactions, *AP-22*, May 1974, pp. 472–475.
2. T. S. Chu and R. H. Turrin, "Depolarization Properties of Offset Reflector Antennas," IEEE Transactions, *AP-21*, May 1973, pp. 339–345.
3. E. A. Ohm, "A Proposed Multiple-Beam Microwave Antenna for Earth Stations and Satellites," B.S.T.J., *53*, No. 8 (October 1974), pp. 1657–1666.
4. E. A. Ohm and M. J. Gans, "Numerical Analysis of Multiple-Beam Offset Cassegrainian Antennas," AIAA Paper #76-301. AIAA/CASI 6th Communication Satellite Systems Conference, Montreal, Canada, April 5–8, 1976.
5. C. Dragone and D. C. Hogg, "Wide Angle Radiation Due to Rough Phase Fronts," B.S.T.J., *42*, No. 7 (September 1963), pp. 2285–2296.
6. P. F. Goldsmith, "A Quasi-Optical Feed System for Radio Astronomical Observations at Millimeter Wavelengths," B.S.T.J., *56*, No. 8 (October 1977), pp. 1483–1501.
7. T. S. Chu and W. E. Legg, "A 19/28.5 GHz Quasi-Optical Feed for an Offset Cassegrainian Antenna," IEEE/APS Symposium, Amherst, Mass., October 1976.
8. J. A. Arnaud and F. A. Pelow, "Resonant-Grid Quasi-Optical Diplexers," B.S.T.J., *54*, No. 2 (February 1975), pp. 263–283.
9. T. S. Chu, M. J. Gans, and W. E. Legg, "Quasi-Optical Polarization Diplexing of Microwaves," B.S.T.J., *54*, No. 10 (December 1975), pp. 1665–1680.
10. I. Anderson, "Measurements of 20 GHz Transmission Through a Radome in Rain," IEEE Transactions, *AP-23*, September 1975, pp. 619–622.
11. C. Dragone, "Reflection and Transmission Characteristics of a Broadband Corrugated Feed: A Comparison Between Theory and Experiment," B.S.T.J., *56*, No. 6 (July-August 1977), pp. 869–888.
12. T. S. Chu, "Geometrical Representation of Gaussian Beam Propagation," B.S.T.J., *45*, No. 2 (February 1966), pp. 287–299.
13. H. Kogelnik and T. Li, "Laser Beams and Resonators," Proc. IEEE, *54*, October 1966, pp. 1312–1329.
14. M. J. Gans and R. A. Semplak, "Some Far-Field Studies of an Offset Launcher," B.S.T.J., *53*, No. 7 (September 1974) pp. 1319–1340.
15. J. S. Cook, E. M. Elam, and H. Zucker, "The Open Cassegrain Antenna: Part 1—Electromagnetic Design and Analysis," B.S.T.J., *44*, No. 7 (September 1965), pp. 1255–1300.

16. H. W. Arnold, D. C. Cox, H. H. Hoffman, R. H. Brandt, R. P. Leck, and M. F. Wazowicz, "The 19 and 28 GHz Receiving Electronics for the Crawford Hill COMSTAR Beacon Propagation Experiment," B.S.T.J., this issue, pp. 1289–1329.
17. C. Dragone, "An Improved Antenna for Microwave Radio Systems Consisting of Two Cylindrical Reflectors and a Corrugated Horn," B.S.T.J., *53*, No. 7 (September 1974), pp. 1351–1377.
18. T. S. Chu and W. E. Legg, "Gain of Corrugated Conical Horns," IEEE/APS Symposium, College Park, Md., May 1978.